State of Charge Estimation and Battery Balancing Control

André Abido Figueiró, Alessandro Jacoud Peixoto and Ramon R. Costa

***Abstract*— In this paper, we propose an algorithm to solve the balancing problem of multi-cell battery systems consisting in the equalization of all cells state of charge (SoC). A nonlinear cell model is presented and experiments are conducted to identify the cell parameters by using a $LiFePO_4$ battery cell. By considering the main cell nonlinear dynamics, ultimate balancing is guaranteed via state feedback. Output feedback versions of the proposed balancing algorithm based on Kalman filtering are evaluated via numerical simulations using the identified model. For the case when the SoC is not available and, in addition, the cell parameters are unknown, a novel SoC/parameter joint estimator is developed for a class of nonlinear cells via amplitude demodulation and online normalized least squares estimation techniques.**

I. Introduction

Battery balancing is of essential importance for multi-cell battery systems since battery characteristic model parameters change with time and operating conditions. Thus, SoC estimation has practical application for battery system management. During a battery operation it can become unbalanced mainly due to physicochemical differences among the cells caused by its production, storage or aging. Without a suitable balancing control system, the cells unbalancing tends to increase and reduce the battery total capacity [1].

The battery balancing control consists in consume the stored capacity in certain cells or transfer the stored capacity among the cells to equalize the battery SoC and, consequently, maximizes the battery total capacity [2]. By using appropriate models for the cell, estimates of the SoC via voltage and current measurements are necessary to implement the cell balancing algorithm. In general, the battery balancing system can be divided in three groups: passive, active and switched balancing. In the passive balancing, resistors or others electronic devices are used to consume charge from specific cells, while DC-DC converters are employed to transfers charge among the cells [3] for the active balancing. The switched balancing connect/disconnect the cells to one or more loads in order to equalize the battery SoC [4].

Several cells models can be found in the literature, from static nonlinear models [5] [6] to dynamic models describing the SoC time evolution due to the cell input current and temperature. When a precise cell model description is required, electrochemical models [7] and neural networks based models [8] become relevant. The dynamic models are, in general, described by means of an equivalent electrical circuit with the current cell as the input, the SoC as one of the system states and the cell voltage as the output. Third order nonlinear equivalent electrical circuits are used in [9], [10], [11] and [12], while a first order nonlinear circuit is considered in [13]. A comparison between models can be found in [5] and [6].

A. A. Figueiró, A. J. Peixoto and R. R. Costa are with the Department of Electrical Engineering, Federal University of Rio de Janeiro, Rio de Janeiro, RJ 45435, Brazil {jacoud,ramon}@coep.ufrj.br (*corresponding author). This work is partially supported by COPPE/UFRJ (Brazil).

In this paper, experiments are conducted on a Li-ion battery pack to identify the cell parameters by using the proposed identification algorithm which is inspired from [14] and [15]. A third order nonlinear electrical cell model is provided. Then, a state feedback balancing control strategy is proposed and its convergence analysis is developed for a class of first order nonlinear cell. It is assured that the battery charge balancing is achieved starting from any initial charge distribution. The control performance is evaluated via numerical simulations considering the nonlinear cell model. Moreover, an output feedback version of the proposed balancing control scheme is also evaluated, where the SoC is estimated by using Unscented and Extended Kalman Filters when the cells parameter are known. For the case when the cells parameters are unknown, a integrated algorithm to simultaneously identify the cell model parameters and SoC is developed for a class of nonlinear first order cells. A periodic perturbation is added to the control current so that the open circuit voltage and cell impedance are estimated by using an amplitude demodulation technique. Subsequently, a normalized least squares and a recursive least squares estimators are employed to obtain the cell parameters and the SoC online. Numerical simulations illustrate the applicability of the proposed SoC/parameter joint estimator. The paper contribution lies in three aspects: (i) the parameter offline identification algorithm, (ii) the battery balancing control scheme and (iii) the joint parameters/SoC online estimator.

A. Notation and Terminology

A cell is *totally charged* (*discharged*) when the steady state open circuit voltage in its terminals (OCV) reaches the maximum (minimum) limit, which is determined by the cell manufacturer. The voltage in the cell terminals depends on the chemical composition of the electrolyte, cathode and anode [16]. For practical reasons a group of cells connected in parallel are treated as a single cell. A *battery* is considered as a group of cells connected in series. A cell *total capacity* (in **Ah**) stands for the amount of charge which can be supplied from the cell between the totally charged and totally discharged states, without recharging or balancing. The *stored charge* (in **Ah**) of a cell is the maximum charge it can supply until it is totally discharged, without being recharging. The *usable charge* (in **Ah**) of a cell is the maximum charge it can supply between the totally charged and totally discharged states, without being recharged or balanced. A cell *state of charge* (dimensionless), denoted by SoC, stands for the relation between the stored charge in a cell and its total capacity. The symbol "s" represents either the Laplace variable or the differential operator "d/dt", according to the context. The output y of a linear time invariant (LTI) system with transfer function $H(s)$ and input u is denoted by $y = H(s)u$.

II. Battery Cell Model

The first issue related to battery balancing is the cell description using a dynamic model. The cell dynamic model must relate the cell SoC with the cell current and the voltage in the cell terminals. Here is presented a third order dynamic model inspired in [11], although, it is important to note that other models are available in literature [5].

Initially, we represent the cell equivalent output impedance by a second order dynamic system composed by two parallel RC-circuits, both represented in Figure 1, with resistances R_1 and R_2 (in Ω) and capacitances C_1 and C_2 (in F). The states x_1 and x_2 are the capacitors voltages. Such dynamics is a simplified representation of the main physical and chemical phenomena, such as the ions transport in the cell [17].

The two RC-dynamics with states x_1, x_2 (capacitor voltage) are given by:

$$\dot{x}_1 = -\frac{1}{R_1C_1}x_1 + u\frac{1}{C_1}, \tag{1}$$

$$\dot{x}_2 = -\frac{1}{R_2C_2}x_2 + u\frac{1}{C_2}, \tag{2}$$

where u is the input current. Let x_3 be the voltage across the capacitor C_3 (in F), not shown in Figure 1. Then, it is clear that the x_3-dynamics can be written as $\dot{x}_3 = \frac{u}{C_3}$. Recalling that SoC is the defined as the quotient of the stored charge in a cell, C_3x_3, and its total capacity

$$Q := C_3x_3|_{x_3=1V}, \tag{3}$$

one has that

$$SoC := \frac{C_3x_3}{Q} \tag{4}$$

is a dimensionless quantity. For $0 \leq x_3 \leq 1$, the cell SoC is physically limited between 0 (or 0 %) and 1 (or 100 %). A zero percent SoC (0 %) corresponds to the capacitor C_3 be fully discharged. On the other hand, SoC equal to 100 % corresponds to the capacitor C_3 be fully charged.

From (3), it is clear that Q is numerically equal to C_3, i.e., $Q = C_3$. Hence, from (4) one can conclude that x_3 and SoC are also numerically equal and we say that x_3 represents the SoC of the battery quantitatively. In fact, since $\dot{x}_3 = \frac{u}{C_3}$, from (4) one can write $\frac{d}{dt}(SoC) = u/Q$. Moreover, allowing an abuse of notation and without lost of generality, in what follows we assume that $x_3 \equiv SoC$, so that the x_3-dynamics can be written as

$$\dot{x}_3 = \frac{u}{Q}. \tag{5}$$

Finally, the cell output voltage y is described by:

$$y = E(x_3) - R_3u - x_1 - x_2, \tag{6}$$

where $E(x_3)$ is the cell steady state OCV (when $x_1 = x_2 = 0$), expressed in V, and R_3 is expressed in Ω. The steady state OCV, $E : \mathbb{R}^+ \to \mathbb{R}^+$, is a positive, continuous and increasing function given by $E(x_3) = \beta_0 + \beta_1/(x_3 + \beta_2)$, with β_i $(i = 1, 2, 3)$ being appropriate constants.

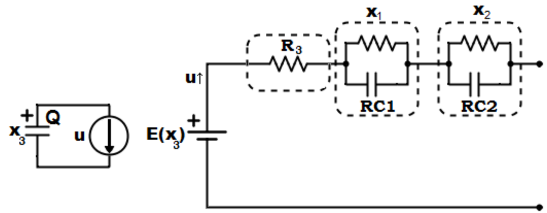

Fig. 1: Battery cell electrical model.

By considering the state vector $X := [x_1\ x_2\ x_3]^T$, the state-space representation is given by:

$$\dot{X} \;=\; AX + Bu, \quad y = \mathscr{H}(X, u), \tag{7}$$

with $A = \begin{bmatrix} -\frac{1}{R_1C_1} & 0 & 0 \\ 0 & -\frac{1}{R_2C_2} & 0 \\ 0 & 0 & 0 \end{bmatrix}$, $B = \begin{bmatrix} \frac{1}{C_1} \\ \frac{1}{C_2} \\ \frac{1}{Q} \end{bmatrix}$ and $\mathscr{H}(X, u) = E(x_3) - x_1 - x_2 + R_3u$.

A. First Order Simplified Model

A simplified cell model can be designed as a first-order dynamic system with the SoC as the model state. The SoC-dynamics is the same as in (5), see Figure 2, where $E(x)$ is the cell OCV and R is the cell equivalent series resistance. Thus, the SoC-dynamics can be represented by

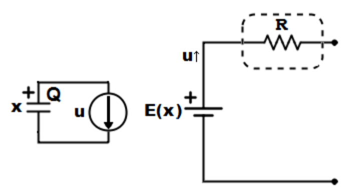

Fig. 2: Battery cell simplified electric model.

$$\dot{x} = \frac{u}{Q}, \tag{8}$$

where $x = SoC$ is the state vector, u is the plant input (cell current) while the cell voltage y (output) is described by

$$y(t) = E(x) - Ru, \tag{9}$$

with the OCV $E : \mathbb{R}^+ \to \mathbb{R}^+$ being a positive, continuous and increasing function given by

$$E(x) = \beta_0 + \frac{\beta_1}{x_3 + \beta_2}. \tag{10}$$

III. Battery Cell Parameters Identification

The test bench for the cells consists on a microcontroller driving a power supply which charges or discharges the $LiFePO_4$ battery cell with current pulses. The microcontroller generates a current pulse train with a definite duration $t_p = 60s$, amplitude i_p and open circuit vanishing time $t_r = 60s$ (zero current) after each current pulse. Note that, after n completed pulses, the integral of the current pulses (Q_p) is given by:

$$Q_p = t_p i_p n \,. \tag{11}$$

Therefore, if the experiment starts at a known battery SoC, it is possible to obtain the battery SoC for each subsequent moment from (11). Indeed, from (5) and considering u given by the pulse train, one has that:

$$x_3(t) = x_3(0) + (t_p i_p n)/Q \,. \tag{12}$$

Besides controlling the current pulses the microcontroller also acquires the cell voltage at a constant sampling rate. The measured values are transmitted to a computer via a serial interface and stored for posterior analysis.

A. Steady State Analysis

It is important to conduct the experiments by charging and discharging the cell, measuring the cell voltages during the current pulses and in the pulses intervals [10]. After each pulse transition, a time delay $t_\Delta = t_p - 1 = 59s$ is considered before the output voltage acquisition in order to allow the RC circuits dynamics reach their steady state. Then, the voltage measurement is acquired at $t = k(t_p + t_r) + t_\Delta$ (during the pulse with amplitude i_p and duration t_p) and at $t = k(t_p + t_r) + t_p + t_\Delta$ (during the zero current interval with duration t_r), where $k = 0, 1, \ldots$ corresponds to the k-th pulse. The amplitude for the charging pulse is $i_p = -674mA$ and for the discharging pulse is $i_p = 757mA$.

The experimental data set is illustrated in Figure 3. By

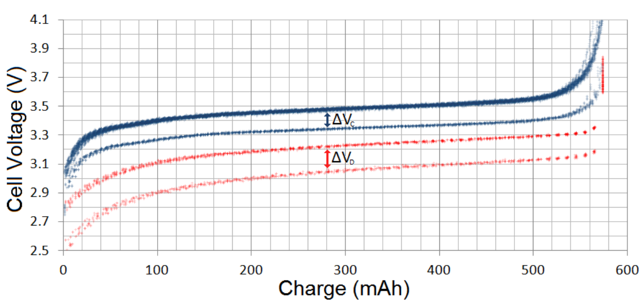

Fig. 3: Voltage experimental data $y(t)$ for a $LiFePO_4$ cell as a function of the cell SoC $x_3(t)$, for the time instants $t = k(t_p + t_r) + t_\Delta$ and $t = k(t_p + t_r) + t_p + t_\Delta$. The charging cycle is in blue solid line, while the discharge cycle is represented in red dash-dot line.

reminding that the *total cell capacity* (Q) stands for the amount of charge which can be supplied from the cell between the totally charged and totally discharged states, then Q can be determined as follows. The cell is full charged and then it is full discharged by applying the current pulse train so that $Q = Q_p$, resulting in $Q = 2070C$. The SoC of 100% and 0% can be detected by measuring the cell OCV and comparing with corresponding OCV limits, which are known *a priori* by the manufacturer datasheet (in this case 2.5V and 4.1V). Thus, starting at the full charge SoC and considering (12), we can obtain the cell SoC $x_3(t)$, $\forall t$.

During the zero current pulse and after the time delay t_Δ, at $t = k(t_p + t_r) + t_p + t_\Delta$, we acquire the output voltage $y(t)$ and use the SoC $x_3(t)$ from (12). Then, the function $E(x_3)$ can be directly identified from (6) and using least squares [6]. Indeed, from (6) one can write (for $k = 0, 1, \ldots$):

$$y(t) = E(x_3(t))\,, \quad t = k(t_p + t_r) + t_p + t_\Delta\,, \tag{13}$$

by noting that $u(t) = 0$ and, therefore, the term $-R_3 u(t) - x_1(t) - x_2(t)$ in (6) can be neglected since the time delay t_Δ was designed large enough to assure that $x_1(t)$ and $x_2(t)$ achieve their steady state values $x_{1ss} = x_{2ss} = 0$. Hence, by using least squares the following estimate for the function $E(\cdot)$ is obtained:

$$\hat{E}(x_3) = \hat{\beta}_0 + \frac{\hat{\beta}_1}{x_3 + \hat{\beta}_2}\,, \tag{14}$$

where the parameters are: $\hat{\beta}_0 = 3.37$, $\hat{\beta}_1 = -0.09$ and $\hat{\beta}_2 = 0.115$.

Analogously, during the current pulse with amplitude i_p and at $t = k(t_p + t_r) + t_\Delta$, we acquire the output voltage $y(t)$, use the SoC $x_3(t)$ in (12) and the identified function $\hat{E}(\cdot)$ in (14). Then, the equivalent series resistance $R = R_1 + R_2 + R_3$ can be directly identified from (6). Indeed, from (6) one can write (for $k = 0, 1, \ldots$):

$$y(t) = \hat{E}(x_3(t)) - R i_p\,, \quad t = k(t_p + t_r) + t_\Delta\,, \tag{15}$$

by noting that $u(t) = i_p$, and, therefore, the term $-R_3 u(t) - x_1(t) - x_2(t)$ in (6) is given by $-R_3 i_p - R_1 i_p - R_2 i_p$ since the time delay t_Δ was designed large enough to assure that $x_1(t)$ and $x_2(t)$ achieve their steady state values $x_{1ss} = R_1 i_p$ and $x_{2ss} = R_2 i_p$. The resistance $R = 0.2\Omega$ is obtained by applying least squares to (15).

B. Transient Analysis

For the transient analysis we use the cell voltage measurements at the beginning of the charging cycle, just after a full discharge. The amplitude for the charging pulse is $i_p = -400mA$ and for the discharging pulse is $i_p = 1008mA$. The time constants of the RC-circuits, $\tau_i = 1/R_i C_i$ $(i = 1, 2)$, were estimated from the response illustrated in Figure 4, by using the transient information. The identified parameters are: $\tau_1 = 69s$, $\tau_2 = 27s$, $R_1 = 0.115\Omega$, $R_2 = 0.066\Omega$ and $R_3 = R - (R_1 + R_2) = 0.174\Omega$.

IV. Balancing Problem Formulation

Consider the simplified cell model presented in (II-A). The battery system model is composed by a group of N cells connected in series. Each cell is modeled by a first-order model, having capacity Q and a series equivalent resistance

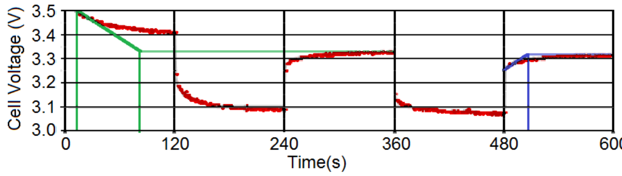

Fig. 4: Voltage experimental data for a $LiFePO_4$ cell as a function of time used to estimate the *RC* circuits parameters.

R. Their SoCs are represented by x_i $(i = 1,\ldots,N)$ while the current for each cell is denoted by u_i and the cell voltage is denote by y_i. Therefore, the battery system is written as:

$$\dot{x}_i = \frac{u_i}{Q}, \quad y_i = E(x_i) - Ru_i\,. \tag{16}$$

The balancing algorithm is designed to bring the SoC of all cells connected in series to a same value. This problem can be faced as a tracking problem by setting the desired SoC, $x_d(t)$, to be either the mean SoC among all cells or the minimum SoC, at a time t. The **tracking error** is defined by

$$e_i := x_d - x_i\,, \quad i = 1,\ldots,N\,, \tag{17}$$

where the desired signal x_d will be defined later on. The passive balancing is considered. In this method, the charge difference responsible for the unbalance is dissipated in a design resistor R_b. The **control objective** consists in finding a passive control signal such that the tracking error tends to zero as $t \to \infty$.

Now, consider the following assumption:

(A1) The battery is connected to a load so that the discharging current I satisfies $I < E(0)/R$.

Note that, since $E(\cdot)$ is a increasing function, Assumption **(A1)** assures that

$$E(x_i) > RI\,, \forall x_i \geq 0\,,\ (i = 1,\ldots,N)\,. \tag{18}$$

Note that **(A1)** is not restrictive, since a rough estimate of the minimum value of the OCV ($E(0)$) and of the equivalent series resistance (R) is always available so that one can design I to satisfy the inequality given in **(A1)**.

V. Passive Balancing Control Scheme

Without lost of generality, assume that entire battery is discharging through a load sinking the constant current I. The proposed *control law* is given by:

$$\begin{aligned} u_i &= I + v_i\,, \quad \text{with} \\ v_i &= \begin{cases} 0, & \text{if} \quad e_i \geq 0\,, \\ R_b^{-1} y_i\,, & \text{if} \quad e_i < 0\,. \end{cases} \end{aligned} \tag{19}$$

Considering the error e_i, the cells are separated in the following two groups: $J = \{j \in \mathscr{I}\ | x_j \leq x_d\}$ and $K = \{k \in \mathscr{I}\ | x_k > x_d\}$, where $\mathscr{I} := \{1,\ldots,N\}$. From (16), we obtain the following closed-loop system:

$$Q\dot{x}_i = \begin{cases} I\,, & i \in J\,, \\ R_b^{-1} y_i + I\,, & i \in K\,. \end{cases} \tag{20}$$

Thus, the error dynamics is given by:

$$\dot{e}_i = \begin{cases} \dot{x}_d - I/Q\,, & i \in J\,, \\ \dot{x}_d - \left(R_b^{-1} y_i + I\right)/Q\,, & i \in K\,. \end{cases} \tag{21}$$

A. Stability Analysis

Two different approaches were used for passive balancing depending on the choice of the reference signal x_d. The first approach uses the mean SoC among all cells as the desired value x_d. The cells with SoC greater than the mean are discharged by a resistor R_b. The second approach uses the minimum SoC among the cells as the desired value x_d. In this case, any cells with SoC different from x_d is discharged by a resistor R_b.

In the **first approach**, the reference signal is given by:

$$x_d := \frac{1}{N}\sum_{i=1}^{N} x_i\,, \tag{22}$$

while, in the **second approach**, the reference signal is redefined as

$$x_d := \min\{x_1,\ldots,x_N\}\,. \tag{23}$$

The main results are summarized in what follows.

Theorem 1: Consider the uncertain linear system (16) with control law (19) and tracking error e_i in (17).(A1) holds. Then, for both balancing approaches, the e_i-dynamics (21) is asymptotically stable.

Proof: Consider the following *Lyapunov* function and the corresponding time derivative along the solution of (21):

$$2V = \sum_{i=1}^{N} e_i^2\,, \quad \dot{V} = \sum_{i=1}^{N} e_i \dot{e}_i\,. \tag{24}$$

From (21), one can rewrite $\dot{V}$ in (24) as:

$$\dot{V} = (\dot{x}_d - I/Q)\sum_{i=1}^{N} e_i - \sum_{i\in K} e_i R_b^{-1} y_i/Q\,. \tag{25}$$

For the *first approach*, by the definition of x_d in (22) and remiding that $e_i = x_d - x_i$, one can verify that $\sum_{i=1}^{N} e_i = N x_d - \sum_{i=1}^{N} x_i = 0$. Therefore, one can further write:

$$\dot{V} = -\sum_{i\in K} e_i R_b^{-1} y_i/Q\,. \tag{26}$$

From (16), (19) and reminding that $u_i = v_i + I$ one can obtain

$$y_i = \frac{E(x_i) - RI}{1 + RR_b^{-1}}\,, \quad i \in K\,, \tag{27}$$

$$y_i = E(x_i) - RI\,, \quad i \in J\,. \tag{28}$$

Moreover, from Assumption **(A1)** and (18), $E(x_i) > RI\,, \forall x_i$. Hence, (27) and (28) imply that $y_i > 0$, $\forall i \in \mathscr{I}$. Finally, from (26) one can obtain $\dot{V} < 0$, since $e_i > 0$, $\forall i \in K$, leading to the conclusion that the closed loop error dynamics is asymptotically stable, starting from any initial SoC.

For the second approach, the control law is also given by (19), but x_d is given by the minimum value of the cells SoC, according to (23). Then, $x_d = x_j$, $\forall j \in J$ and, consequently,

$e_j = 0$, $\forall j \in J$. Hence, the time derivative $\dot{V}$ in (25) also satisfies (26) and, following the same steps for the case where x_d is given by the mean value (22), one can also demonstrate that the closed loop error dynamics is asymptotically stable, starting from any initial SoC. ■

B. State Feedback Passive Balancing: Simulation Results

Numerical simulations were conducted to evaluate the proposed battery balancing control scheme. For the state feedback scheme, a battery modeled by four equal first-order cells connected in series. The cells were initialized with different SoC, named: 98%, 90%, 80% and 70%.

The cell parameters (capacity, equivalent resistance and OCV) were obtained experimentally, according to Section III. The main discharge current I results from a 465Ω discharge resistor connected between the battery terminals, while the balancing control current v_i results from a 93Ω control resistor which is connected or disconnected from the cell, according to each balancing algorithm.

Figure 5 illustrates the closed loop performance with the minimum and mean SoC tracking reference balancing algorithm. Both algorithms balances the battery (all cells with the same SoC) after the same amount of time, and the cells with maximum and minimum SoC time variations are similar. The most significant difference is the number of control switchings (balancing current turning on and off) until the balance occurs.

Remark 1: (**Cells Models of Third Order**) The time constants of the RC-circuits were estimated in Section III-B from the step response and it was observed that it corresponds to a fast dynamics which can be neglected. Indeed, both control balancing strategies were applied to cells with third-order dynamics and no significant difference was observed (curves not shown).

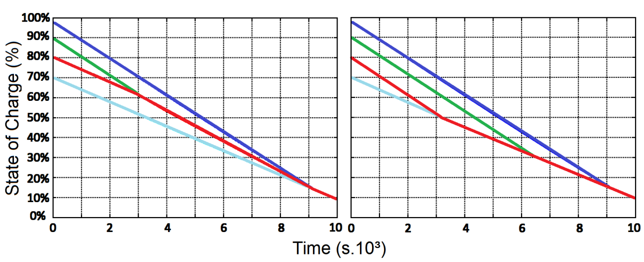

Fig. 5: SoC for the four cells in time for the minimum (left) and mean (right) SoC battery balancing. Note that the initial SoC are different to simulate battery unbalancing

C. Output Feedback Passive Balancing: Simulations Results

In this section, we consider the third order model for the battery cells. The cell SoC is obtained via Extended Kalman Filter (EKF) or Unscented Kalman Filter (UKF), assuming that all the model parameters are **known**. Since both filters operate in discrete-time, the third order cell model (7) is discretized by using the zero-order hold method with sample period $T = 0.1s.$, resulting in:

$$x_t = \Phi x_{t-1} + \Gamma u_t\,, \quad y_t = \mathscr{H}(x_t, u_t)\,, \tag{29}$$

with $\Phi = e^{AT}$ and $\Gamma = \int_0^T e^{As} ds B$. The EKF consists on a recursive estimator for the system state x_t which uses a first order Taylor series approximation for the output function $\mathscr{H}(x_t, u_t)$. The second estimator used is the UKF which uses the unscented transform [18] to calculate the output random variable moments (medium and variance) needed for the gain adaptation.

In order to evaluate the EKF and UKF estimators performance in the output feedback balancing scheme, both (minimum and mean value) SoC balancing approaches were considering in the following numerical simulations, where the estimators initial conditions are: $\hat{x}_1 = 0.01$, $\hat{x}_2 = 0.01$ and $\hat{x}_3 = 0.5$. The same cells SoC initial condition as in the state feedback case is considered, named: 98%, 90%, 80% and 70 %. The cell model parameters were also the same as the ones used in the state feedback case.

The EKF and UKF estimated states for the minimum value SoC tracking balancing are shown in Figure 6. It is clear that the UKF estimator based output feedback battery balancing control scheme presents better results when compared with the EKF estimator, since a fast transient is observed. Moreover, no significant difference from the state feedback balancing is noted since both estimators time convergence are faster than the balancing transient. The same conclusion can be obtained by using the mean SoC tracking balancing approach (curves not shown).

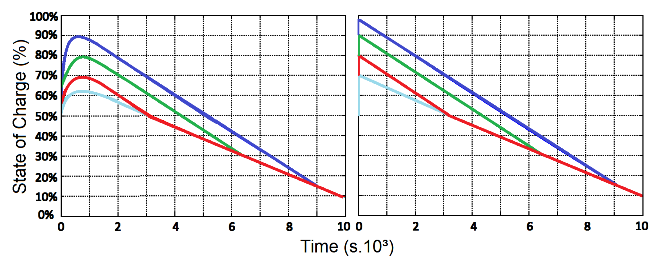

Fig. 6: Estimated states of charge for the four cells in time with minimum SoC tracking balancing. The EKF estimator (left) and UKF estimator (right) are used .

VI. SoC and Model Parameters Estimator

In this section not only the cell states but also the cell parameters are estimated. As in [19], consider the first order model (see also Section (II-A)):

$$\dot{x} = \frac{u}{Q}\,, \tag{30}$$

where x is the cell SoC, Q is the cell capacity and u is current thought the cell. At each time instant t, the SoC satisfies:

$$x(t) = \mathscr{X} - \frac{\lambda}{Q} \tag{31}$$

where $x(0) = \mathscr{X}$ is the SoC initial value and

$$\lambda(t) = \int_0^t u(\tau) d\tau\,, \tag{32}$$

is an **available** signal. The cell voltage y is the following function of the cell SoC x and the current u:

$$y(t) = h(t) - g(t)u(t)\,, \tag{33}$$

where the OCV $h(t)$ and the cell impedance $g(t)$ are the time varying **unknown** signals:

$$h(t) = E_0 + KQ - \frac{K_h Q}{x(t)+\varepsilon} \tag{34}$$

and

$$g(t) = R + \frac{K_g}{x(t)+\varepsilon}\,, \tag{35}$$

respectively, where E_0 is full charge cell OCV, K_h, K_g, K are constants related to the OCV and impedance dependence on the SoC, R is the equivalent cell resistance and ε is a constant required to model the fact that some residual OCV results when the cell is completely discharged ($x = 0$). Note that, this model was extracted from [19] and can be viewed as a generalization of the first order nonlinear model (8). In fact, one has that both model are equivalent by setting $K_g = 0$ and the OCV $E(x)$ in (10) with $\beta_0 = E_0 + KQ$, $\beta_1 = -K_h Q$ and $\beta_2 = \varepsilon$. In what follows, and in accordance with [19], let $K_g = K_k = K$ and $\varepsilon = 0$. Note that, as in [19], we are assuming that x never reaches zero to avoid cell damage.

It is well known that the SoC estimation via model-based estimators can suffer from parameters uncertainties, in particular, when the model parameters change in time due to the phenomenon known as cell aging [12]. Here, we consider the problem of estimating both the model parameters and the SoC, named as *Dual Estimation*. Different approaches can be used to develop a cell dual estimator, such as the Dual Extended Kalman Filter [20], Adaptative Extended Kalman Filter [21] or Neural Networks [8].

In [19], a dither (noise) signal is added to the input cell current so that the cell OCV (h) and its impedance (g) can be estimated in a set of discrete time instants by using statistical moments of the cell output voltage signal (y), its mean and variance. Subsequently, all the cell's parameters are estimated of line via least square.

Here, differently from [19], an online estimator is proposed. The noise dither signal is replaced by a sinusoidal signal with known frequency ω and amplitude (a), i.e, a low amplitude high frequency signal is added to the input cell current. Then, the output cell voltage can be interpreted as an amplitude modulated signal. Hence, a demodulation algorithm is employed to estimate the cell OCV (h) and its impedance (g). These estimates drive a continuous time Normalized Least Squares Estimator which generates online estimates of the cell parameters. Moreover, a discrete time Recursive Least Squares Estimator is also considered.

A. Proposed OCV and Impedance Estimator

To estimate the cell OCV and impedance, a sinusoidal signal $a\sin(\omega t)$ is added to the main input current I resulting in the effective cell current $u(t) = I(t) + a\sin(\omega t)$. Thus, from (33), the cell voltage y satisfies

$$y(t) = [h(t) - g(t)I(t)] + [-ag(t)]\sin(\omega t)\,, \tag{36}$$

and can be viewed as a modulated amplitude signal $y(t) = \alpha_2(t) + \alpha_1(t)\sin(\omega t)$, with $\alpha_1 := -ag(t)$ being the modulated signal, $\sin(\omega t)$ being the carrier and $\alpha_2 := h(t) - g(t)I(t)$ being the mean value. The cell OCV ($\hat{h}$) and impedance $\hat{g}$ estimates are then obtained by the demodulation scheme illustrated in Figure 7 and explained in what follows.

Amplitude and Mean Value Estimator

The amplitude α_1 can be estimate by

$$\hat{\alpha}_1 = \frac{2}{\tau s+1}\left[\sin(\omega t)\eta(t)\right]\,, \tag{37}$$

where τ is a positive design constant and z is the output of the high pass filter

$$\eta = \frac{\tau s}{\tau s+1} y = y - \frac{1}{\tau s+1} y = y - \hat{\alpha}_2\,, \tag{38}$$

where the estimate $\hat{\alpha}_2$ of the mean value α_2 is defined as

$$\hat{\alpha}_2 = \frac{1}{\tau s+1} y\,. \tag{39}$$

Therefore, the cell OCV ($\hat{h}$) and impedance ($\hat{g}$) estimates are given by:

$$\begin{aligned}
\hat{g}(t) &= -\hat{\alpha}_1(t)/a\,, & (40)\\
\hat{h}(t) &= \hat{\alpha}_2(t) + \hat{g}(t)I(t) = \hat{\alpha}_2(t) - \hat{\alpha}_1(t)I(t)/a\,. & (41)
\end{aligned}$$

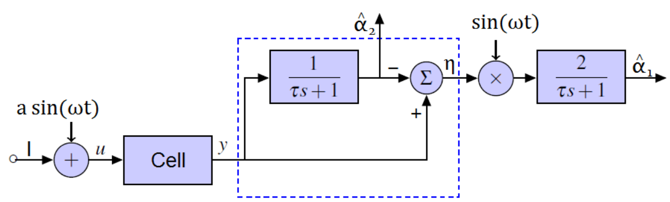

Fig. 7: Cell OCV ($\hat{h}$) and impedance ($\hat{g}$) proposed estimator. The estimates $\hat{h}$ and $\hat{g}$ are obtained from $\hat{\alpha}_1$ and $\hat{\alpha}_2$, according to (40).

Remark 2: (Approximated Analysis) The high pass filter $\frac{\tau s}{\tau s+1}$, applied to the output in the form $y = \alpha_1(t)\sin(\omega t) + \alpha_2(t)$, serves to remove $\alpha_2(t)$, i.e., $\frac{\tau s}{\tau s+1} y \approx \alpha_1(t)\sin(\omega t)$. This signal is then "demodulated" by multiplication with $\sin(\omega t)$ giving $\alpha_1(t)\sin^2(\omega t)$. Now, since $2\sin^2(\omega t) = 1 - \cos(2\omega t)$ only the mean value pass through the law pass filter $\frac{2}{\tau s+1}$. The mean value α_2 is directly estimated via the first order filter $\hat{\alpha}_2 = \frac{1}{\tau s+1} y$, hence, $\hat{\alpha}_1 \approx \alpha_1$ and $\hat{\alpha}_2 \approx \alpha_2$. ■

B. Parameters Estimator

From (31), (32), (34) and (35) one can write:

$$\lambda(t)h(t) = \lambda(t)\Theta_2 + h(t)\Theta_3 + \Theta_4\,, \tag{42}$$

$$\lambda g(t) = \lambda(t)\Theta_1 + g(t)\Theta_3 + \Theta_5\,, \tag{43}$$

where the unknown constants $\Theta_1, \ldots, \Theta_5$ are defined as:

$$\begin{aligned}
\Theta_1 &:= R\,, \quad \Theta_2 := E_0 + KQ\,,\\
\Theta_3 &:= \mathscr{X}Q\,, \quad \Theta_4 := -(E_0 + KQ)(\mathscr{X}Q) - KQ^2\,,\\
\Theta_5 &:= -R(\mathscr{X}Q) - KQ\,. & (44)
\end{aligned}$$

Now, by defining

$$\Theta := [\Theta_1, \ldots, \Theta_5]^T, \quad z(t) := [\lambda(t)h(t),\ \lambda(t)g(t)]^T \quad (45)$$

and

$$H(t) := \begin{bmatrix} 0 & \lambda(t) & h(t) & 1 & 0 \\ \lambda(t) & 0 & g(t) & 0 & 1 \end{bmatrix}, \quad (46)$$

one can rewrite (42) and (43) as:

$$z(t) = H(t)\Theta. \quad (47)$$

Under the ideal condition of accurate values on $g(t)$ and $h(t)$, the unknown parameter Θ is to be calculated as the solution of (47). In reality, the true value of $H(t)$ and $z(t)$ is not available. In fact, H and z are estimated by using $\hat{g}$ and $\hat{h}$ defined in (40). Thus, the goal is to approximate the unknown parameter Θ by the solution θ of

$$\hat{z}(t) = \hat{H}(t)\theta, \quad (48)$$

where

$$\hat{H}(t) := \begin{bmatrix} 0 & \lambda(t) & \hat{h}(t) & 1 & 0 \\ \lambda(t) & 0 & \hat{g}(t) & 0 & 1 \end{bmatrix}, \quad (49)$$

and

$$\hat{z}(t) := [\lambda(t)\hat{h}(t),\ \lambda(t)\hat{g}(t)]^T. \quad (50)$$

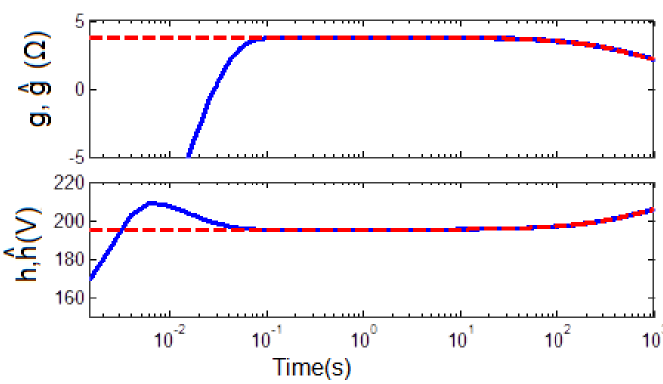

Fig. 8: Cell impedance g (above) and OCV h (bellow) real values (red dotted line) and its estimates (blue solid line).

In what follows, a normalized least squares estimator (NLS) is employed to obtain an estimate $\hat{\theta}$ for the solution θ of (48) and, consequently, an estimate for Θ in (47).

Normalized Least Squares Estimator

Before implementing the NLS estimator, consider the following decomposition of (48):

$$\hat{z}_a = \hat{\phi}_a\theta_a, \quad \hat{z}_b = \hat{\phi}_b\theta_b, \quad (51)$$

where

$$\theta_a = [\theta_2, \theta_3, \theta_4]^T, \quad \theta_b = [\theta_1, \theta_3, \theta_5]^T, \quad (52)$$

$$\hat{z}_a = \hat{h}\lambda, \quad \hat{z}_b = \hat{g}\lambda, \quad (53)$$

$$\hat{\phi}_a = \begin{bmatrix} \lambda & \hat{h} & 1 \end{bmatrix} \quad \text{and} \quad \hat{\phi}_b = \begin{bmatrix} \lambda & \hat{g} & 1 \end{bmatrix}. \quad (54)$$

The estimate $\hat{\theta}_a$ for θ_a and $\hat{\theta}_b$ for θ_b is obtain by the following NLS estimator [22]:

$$\dot{\hat{\theta}}_i = -P_i\phi_i(\hat{\theta}_i^T\hat{\phi}_i - \hat{z}_i)/m_i^2, \quad \dot{P}_i = -P_i\hat{\phi}_i\hat{\phi}_i^T P_i/m_i^2, \quad (55)$$

with

$$m_i = \sqrt{1 + \kappa_i\hat{\phi}_i^T P_i\hat{\phi}_i}, \quad (56)$$

where κ_i is an adjustable design parameter, $P_i(0) = P_0 = P_0^T > 0$, $\forall t \geq 0$ and $i = a, b$.

Recursive Least Squares Estimator

In what follows, the discrete time version of a continuous time signal $\mu(t)$ is denoted by $\mu_k = \mu(t)|_{t=kT}$ ($k = 0, 1, 2, 3, \ldots$), where T is the sampling period. Then, from (48) one can write:

$$\hat{z}_k = \hat{H}_k\theta, \quad (57)$$

where

$$\hat{z}_k = [\hat{h}_k\lambda_k, \hat{g}_k\lambda_k]^T, \quad (58)$$

and

$$\hat{H}_k = \begin{bmatrix} 0 & \lambda_k & \hat{h}_k & 1 & 0 \\ \lambda_k & 0 & \hat{g}_k & 0 & 1 \end{bmatrix}. \quad (59)$$

The Recursive Least Squares (RLS) estimate $\hat{\theta}_k$ is given by [23]:

$$\hat{\theta}_k = \hat{\theta}_{k-1} + K_k(z_k - H_k\hat{\theta}_{k-1}), \quad (60)$$

$$K_k = P_{k-1}H_k^T(H_kP_{k-1}H_k^T + E)^{-1}, \quad (61)$$

$$P_k = (\mathscr{I} - K_kH_k)P_{k-1}, \quad (62)$$

with $\hat{\theta}_0 = \theta(0)$, $E = \alpha\mathscr{I}$, $0 < \alpha < 1$, $P_0 = P_0^T > 0$, $\forall k \geq 0$ and $\mathscr{I}$ being the identity matrix of appropriate dimension.

Model Parameters Estimation

Finally, with $\hat{\theta}$ available from the NLS or RLS, the model parameters are obtained by:

$$\hat{Q} = \frac{\hat{\theta}_4 + \hat{\theta}_3\hat{\theta}_2}{\hat{\theta}_5 + \hat{\theta}_3\hat{\theta}_2}, \quad \hat{\mathscr{X}} = \hat{\theta}_3\frac{\hat{\theta}_5 + \hat{\theta}_3\hat{\theta}_2}{\hat{\theta}_4 + \hat{\theta}_3\hat{\theta}_2}. \quad (63)$$

The SoC estimate is then obtained from

$$\hat{x}(t) = \hat{\mathscr{X}} - \frac{\lambda}{\hat{Q}}. \quad (64)$$

C. Simulations Results

The actual model parameters used in the numerical simulations are: $Q = 6.5Ah$, $\mathscr{X} = 5\%$, $R = 0.3077\Omega$, $K = 0.1737$ and $E_0 = 216.6V$. The input current signal were applied with $I = -5A$, $a = 0.1A$ and $\omega = 2\pi 10^3 rad/s$. The amplitude/mean estimator is implemented with $\tau = 100/\omega$.The initial condition of both NLS and RLS estimators, $\hat{\theta}(0)$, were obtained from (44) with: $\hat{Q}(0) = 4.2Ah$, $\hat{\mathscr{X}}(0) = 70\%$, $\hat{R}(0) = 0.2\Omega$, $\hat{K}(0) = 0.2$ and $\hat{E}_0(0) = 200V$. The initial covariances are $P(0) = 10^3\mathscr{I}$, where $\mathscr{I}$ stands for the identity matrix, and $\alpha = 1e-6$ were used in the RLS estimator (with 5s of sampling period). Figure 8 illustrates the impedance and OCV estimate $\hat{g}$ and $\hat{h}$ while the parameters and SoC estimates are shown in Figure 9, for both NLS and RLS estimators.

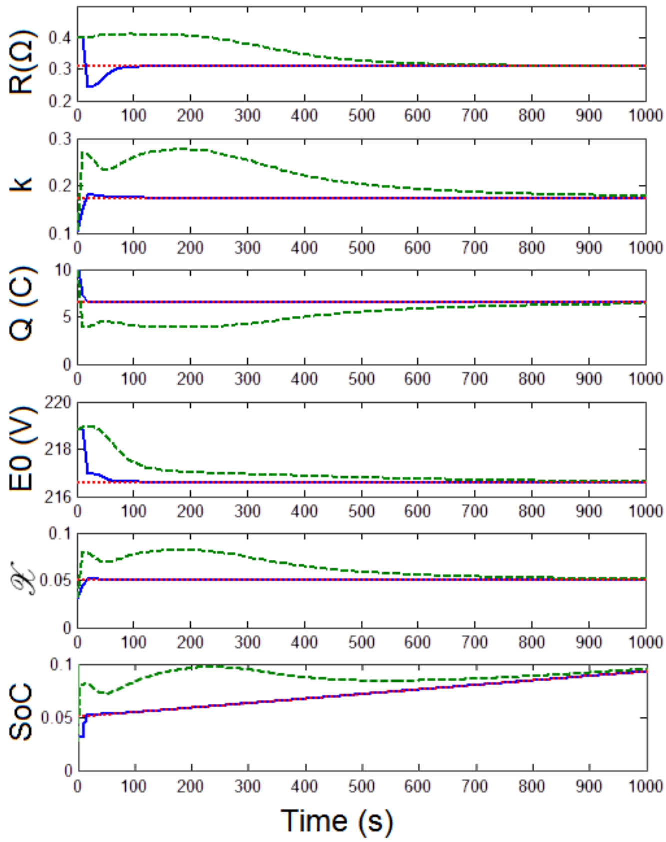

Fig. 9: Cell model parameters and SoC (red dotted line) and the corresponding estimates obtained with the NLS (green dashed line) and RLS (blue solid line) estimators.

VII. Conclusion

A passive balancing control multi-cell battery systems has been proposed to equalize all battery cells state of charge (SoC). The control ideal is to defined the SoC mean or minimum value among all cells as a desired tracking signal. By discharging each cell through a resistance as a function of the tracking error, ultimate balancing is achieved for a class of nonlinear cells. When the SoC is not available for feedback and the cell parameters are unknown, a joint estimator (SoC/parameter) is developed for this class of cells. The estimator combines a demodulation technique for estimating the impedance and open circuit voltage with a normalized least squares technique for obtaining online estimates of the SoC/parameters. Numerical simulations are presented so as to validate the analysis and show the effectiveness of the joint estimation technique. For the case when the cells parameters are known, the balancing algorithm was evaluated via numerical simulations by using Extended and Unscented Kalman Filters for SoC estimation, considering a more elaborate cell model for which the parameters where identified via experiments conducted with a $LiFePO_4$ battery cell. It is important to stress that the strategies of this paper can be extended to different battery types and model structures. The complete stability analysis of the output feedback balancing scheme by considering the proposed joint estimator and the Kalman Filter estimators is a topic of future work. Moreover, the initial condition of the covariances used in the least squares estimators should be carefully selected in order to enhance the algorithm efficiency.

References

[1] H. J. Bergveld, *Battery Management Systems Design by Modelling*, 2001.

[2] W. Bentley, “Cell balancing considerations for lithium-ion battery systems,” *Battery Conference on Applications and Advances, 1997*, pp. 223–226, 1997.

[3] M. Caspar and S. Hohmann, “Optimal Cell Balancing with Model-based Cascade Control by Duty Cycle Adaption,” pp. 10 311–10 318, 2014.

[4] V. Muenzel, J. D. Hoog, M. Brazil, D. A. Thomas, and I. Mareels, “Battery Management using Secondary Loads : A Novel Integrated Approach,” *World Congress of the International Federation of Automatic Control*, pp. 3924–3929, 2014.

[5] H. Hussein and I. Batarseh, “An overview of generic battery models,” *Power and Energy Society General Meeting*, no. 4, pp. 4–9, 2011.

[6] X. Hu, S. Li, and H. Peng, “A comparative study of equivalent circuit models for Li-ion batteries,” *Journal of Power Sources*, vol. 198, pp. 359–367, Jan. 2012.

[7] G. Ning and B. N. Popov, “Cycle Life Modeling of Lithium-Ion Batteries,” *Journal of The Electrochemical Society*, vol. 151, no. 10, p. A1584, 2004.

[8] Y. Shen, “Adaptive online state-of-charge determination based on neuro-controller and neural network,” *Energy Conversion and Management*, vol. 51, no. 5, pp. 1093–1098, May 2010.

[9] R. K. Junnuri, S. Kamat, N. Goyal, R. Annamalai, and D. Modak, “Modelling of HEV Lithium-Ion High Voltage Battery Pack using Dynamic Data Number of Cells,” pp. 6448–6453, 2014.

[10] S. Thanagasundram, R. Arunachala, K. Makinejad, T. Teutsch, and A. Jossen, “A Cell Level Model for Battery Simulation,” *European Electric Vehicle Congress*, no. November, pp. 1–13, 2012.

[11] M. Chen and G. Rincon-Mora, “Accurate electrical battery model capable of predicting runtime and IV performance,” *IEEE Transactions on Energy conversion*, vol. 21, no. 2, pp. 504–511, 2006.

[12] L. Serrao, Z. Chehab, Y. Guezennec, and G. Rizzoni, “An Aging Model of Ni-MH Batteries for Hybrid Electric Vehicles,” *2005 IEEE Vehicle Power and Propulsion Conference*, pp. 78–85, 2005.

[13] O. Tremblay, “A generic battery model for the dynamic simulation of hybrid electric vehicles,” *Vehicle Power and Propulsion Conference*, pp. 284–289, 2007.

[14] S. Lin, H. Zhao, and A. Burke, “A First-Order Transient Response Model for Lithium-ion Batteries of Various Chemistries : Test Data and Model Validation,” 2012.

[15] G. Plett, “Results of temperature-dependent LiPB cell modeling for HEV SOC estimation,” *21st Electric Vehicle Symposium*, no. 1, pp. 1–9, 2005.

[16] MIT Electric Vehicle Team, “A Guide to Understanding Battery Specifications,” no. December, 2008.

[17] D. Di Domenico, G. Fiengo, and A. Stefanopoulou, “Lithium-ion battery state of charge estimation with a Kalman Filter based on a electrochemical model,” *2008 IEEE International Conference on Control Applications*, pp. 702–707, 2008.

[18] R. V. D. Merwe, “Sigma-point Kalman filters for probabilistic inference in dynamic state-space models,” *PhD thesis*, p. 378, 2004.

[19] L. Liu, L. Wang, and Z. Chen, “Integrated system identification and state-of-charge estimation of battery systems,” *IEEE Transactions on Energy conversion*, vol. 28, no. 1, pp. 12–23, 2013.

[20] S. Lee, J. Kim, J. Lee, and B. Cho, “The state and parameter estimation of an Li-ion battery using a new OCV-SOC concept,” *IEEE Annual Power Electronics Specialists Conference*, pp. 2799–2803, 2007.

[21] H. He, R. Xiong, and X. Zhang, “State-of-charge estimation of the lithium-ion battery using an adaptive extended Kalman filter based on an improved Thevenin model,” *IEEE Transactions on Vehicular Technology*, vol. 60, no. 4, pp. 1461–1469, 2011.

[22] G. Tao, *Adaptive control design and analysis*, 2003.

[23] D. Simon, *Optimal State Estimation: Kalman, H-Infinity, and Nonlinear Approaches*, 2006.